Quantification of shrinkage micro-cracking in young mortar with fluorescence light microscopy and ESEM

J. Bisschop and J.G.M. van Mier
Delft University of Technology, Faculty of Civil Engineering and Geo-Sciences ,M2L laboratory, Delft, The Netherlands

In this paper a method is described to quantify shrinkage microcracking in young mortar by means of crack mapping. Visualisation of the microcracks is realised with two techniques: Fluorescence Light Microscopy (FLM) and Environmental Scanning Electron Microscopy (ESEM). The preliminary results obtained with the microcrack mapping method showed an increase in extent of shrinkage microcracking as a function of the hardening time of the young mortar, probably due to autogenous shrinkage. In the ESEM it was observed that microcracks in the young mortar open upon drying from relative humidities of about 25% to 1%. It is concluded in this paper that quantitative microcrack mapping at constant magnification should be done as a function of relative humidity of the sample and its environments.

Keywords: **young mortar, shrinkage microcracking, fluorescence light microscopy, ESEM, crack mapping.**

1 Introduction

During the hardening of young concrete the cement paste shrinks due to hydration and drying processes. The types of shrinkage that can be distinguished at the early ages of concrete are plastic, drying, autogenous, thermal and carbonation shrinkage [1]. These types of shrinkage can lead to initial (micro)cracking when the stresses due to shrinkage exceed the tensile strength of the material. To get more insight in the actual distribution of shrinkage microcracks in concrete or mortar specimens crack mapping can be carried out. Such a structural analysis of the microcracks might elucidate their possible relation to areas with high initial eigenstresses or weak spots in the hardening material. When it has been determined how microcracks are distributed within a mortar specimen as a function of composition and curing conditions, and when the underlying mechanisms have been determined, it might be possible to use these data to develop numerical models that simulate crack growth in concrete from an early stage including the hardening stage.
A number of techniques are available to assess the presence of microcracking in concrete and mortar. The most widely used techniques are (optical) light and electron microscopy. When these techniques are applied to study internal microcracking, the sample preparation is destructive. This may be a drawback, because sample preparation involves cutting and/or drying of the con-

crete, and these preparation actions may introduce unwanted additional microcracks. For example, the study of microcracking in thin- or polished sections with fluorescence light microscopy involves the vacuum-impregnation of microcracks with a fluorescent epoxy. The drying before the impregnation and the impregnation itself may introduce additional microcracks on the sample surface, which would not have been present internally [2,3]. Sample preparation for a conventional scanning electron microscope also involves drying of the concrete, and besides the sample is placed in the high vacuum of the SEM-chamber. Probably the only possibility to study shrinkage microcracking in concrete quantitatively with SEM is by means of the replica-technique [4,5].

A new technique, which can be used to study microcracking in wet or partly saturated concrete and mortar, is environmental scanning electron microscopy (ESEM). ESEM is in most respects similar to conventional SEM, but in ESEM it is also possible to study the concrete in a moist environment. Wet concrete samples can be placed in the ESEM-chamber, and subsequently studied at controlled relative humidities ranging from 0 to 100%. Sujata and Jennings [6] have described the technique in detail. Kjellsen and Jennings [7] have studied microcracks in ESEM, and showed that microcracks open upon drying and close by rewetting in ESEM.

In an on-going study at Delft University of Technology fluorescence light microscopy and ESEM are used to characterise shrinkage microcracking in young mortar. By using this combination of techniques it might become clear whether any damage is introduced during sample preparation. This is important because young mortar may be much more susceptible to sample preparation damage (drying and cutting) than mature mortar.

A method is developed to quantify internal shrinkage microcracking by means of microcrack mapping. The method relies on the two aforementioned microscopic techniques, and it starts with $40 \times 40 \times 160$ mm^3 prisms of young mortar. In this paper a description of the method is given and some preliminary results will be presented.

2 Experimental

2.1 *Materials and specimen conditioning*

The material that is used in this study is a mortar with a water/cement ratio of 0.5 and a sand/cement ratio of 0.5. The used Portland cement is a Dutch (ENCI) industrial cement (CEM I 52.5R) with the following mineralogical composition: C_3S = 63%, C_2S = 13%, C_3A = 8% and C_4AF = 9% (Bogue calculation) and Blaine fineness of 530 m^2/kg. The grain size distribution of the sand (mainly quartz) was: 2-4 mm = 29.3%, 1-2 mm = 20.7%, 0.5-1 mm = 14.6%, and 0.25-0.5 mm = 35.4%. It was added air-dried.

The cement and sand were mixed thoroughly before the demineralised water was added. The complete mixture was then stirred for 3 minutes using a large blade in a 10*l* bowl of a Hobart mixer. The paste was casted in moulds of $40 \times 40 \times 160$ mm^3 and vibrated 10 seconds on a table vibrator. The moulds were sealed with plastic and stored at room temperature for 24 hours. Then the prisms were demoulded and placed in demineralised, portlandite-saturated, and CO_2-poor water. At an age of 48 hours the first part of the prisms were used for microscope sample preparation. Sample preparation of the other set of prisms started at an age of 8 days.

2.2 *Microscope samples preparation*

From each prism 1 fluorescent thin-section and 1 ESEM-sample is made. A total of three thin-section and three ESEM-samples are made at each hardening stage (2 and 8 days). In Figure 1 the preparation procedure of the microscope samples is shown schematically. The thin-section (TS-) sample and ESEM-sample are cut in such a way from the prism that both sample surfaces to be examined are situated as closely as possible in the center of the prism parallel to the casting surface (see Figure 1). The whole procedure is developed in such a way, that the chance of introducing microcracks by preparation is minimized.

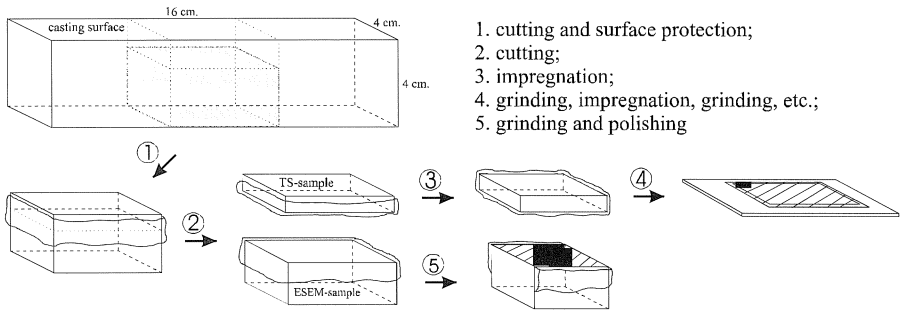

Fig. 1. Procedure for the preparation of fluorescent thin-sections and ESEM-samples (see text for detailed description).

Two thin-sections are made with a number of cuts perpendicular to the final microscope sample surface, with the purpose to check if cutting possibly introduces additional damage.

The sample preparation procedure is as follows (see Figure 1):

1. The $40 \times 40 \times 160$ mm^3 prism is cut along the dotted lines with a diamond saw. After cutting the sample, it is dried for 30 min at 40°C. Then, the surfaces of the sample are protected with plastic padding (see Figure 1). Due to this protection layer the edges of the sample are not damaged during further cutting and grinding.

2. The sample is cut to separate the TS-sample from the ESEM-sample as soon as the plastic padding has hardened. Cutting is done very carefully with a fine (1 mm thick) diamond saw. The ESEM-sample is stored at a relative humidity (r.h.) of 100% until ESEM-sample preparation is continued.

3. The TS-sample is vacuum-impregnated with a fluorescent epoxy after drying for 30 min at 40°C. The purpose of this impregnation stage is to impregnate weak porous zones around the sand grains and air-voids. The TS-sample surface gains some extra strength and the chance of introducing damage during the first grinding stage reduces in comparison to a sample which was not impregnated. The impregnated sample is stored for 6 hours at 40°C in an oven to let the epoxy harden.

4. To produce the thin-sections a diamond roller grinder/86 designed by Dansk Beton Teknik is used. The equipment is particularly suited for the production of thin-section specimens in connection with microscopic structural analysis of concrete [8]. After the first impregnation the edges of the sample are cut to make the sample fit on the microscope slide. Then, the sample is ground to produce a flat surface. This grinding is followed by a second impregnation stage with fluorescent epoxy after drying the sample 30 min at 40°C. In this stage microcracks, pores, and voids are impregnated. After the epoxy has hardened the excess of epoxy is removed by grinding. Then, the sample is glued on the microscope glass. Part of the TS-sample is cut away and the thin-section is ground to a thickness of 30 μm. Finally, the thin-section is finished by covering it with a cover glass.

5. The edges of the ESEM-sample are cut away to keep the sample surface small for polishing purposes. The ESEM-sample is ground by hand with moderate pressure on a moderate-speed lap wheel with sand papers of p230, p500, and p1200, respectively. This is followed by polishing by hand on a Struers low-speed lap wheel covered with a DP polishing cloth. We used series of 6, 3, 1, and 0.25 μm diamond pastes (1 min per diamond paste) and demineralised water as a polishing agent. No alcohols were used during any stage of the thin-section or the ESEM-sample preparation. The ESEM-samples are stored at a relative humidity of 100% until they are viewed in the ESEM.

It should be noted that during thin-section production the drying time of the mortar is always 30 min at 40°C. The measured relative humidity in the oven was in between 20 and 40%. So, during the sample preparation hydration probably can proceed within the sample. The microcrack pattern in the thin-section is 'frozen in' during the second impregnation stage at an age of 58 hours and 202 hours for the two hardening stages, respectively. The ESEM-samples surface are never dried (only in the ESEM) and hydration can proceed in the samples. The three ESEM-samples are viewed in the ESEM at ages of 73, 75, and 77 hours (2 hours per sample) at the first hardening stage and at ages 217, 219, and 221 hours at the second hardening stage. The total sample area of both the TS- and the ESEM-sample is 40×35 mm^2.

2.3 *Microscopes*

The microscope samples are studied with a light and electron microscope present at the M2L Laboratory at the Faculty of Civil Engineering and Geo-Sciences at Delft University of Technology. The fluorescent thin-sections are examined with a Leica transmitted light microscope with a fluorescent light mode. Reference images of both microscope sample types are made using a CCD-camera connected onto a Leica reflected light stereomicroscope (5–40×), also with a fluorescent light mode. The polished ESEM-samples are examined in a Phillips XL30 ESEM-W using two types of detectors. Firstly, a so-called Gaseous Secondary Electron (GSE) detector is used, which is the 'wet-mode' SE-detector of ESEM. This detector can be used at water vapour pressures in the ESEM-chamber between 0 and 10 torr. Secondly, a low-vacuum Backscatter Electron (BSE) detector is used. This detector can be used at chamber pressures between 0 and 2 torr.

3 Crack quantification method

3.1 *Appearance of microcracks in fluorescent thin-sections*

In fluorescent thin-sections microcracks are filled with the fluorescent epoxy. The contrast of the impregnated microcracks with the adjacent material strongly depends on the porosity of the cement paste. In HPC for example, the porosity is relatively low, and this causes a high contrast of the microcracks, because there is only a minor amount of epoxy in the paste [3]. In the mortar used in this study, the porosity is relatively high and the impregnated paste fraction is also very illuminating. Consequently, the contrast of the microcracks can be very low locally. It is possible that microcracks, especially small ones (< 1 μm width), are not detected due to this lack of contrast.
In general, two types of microcracks are observed in the examined fluorescent thin-sections. Firstly, microcracks in the interfacial zone between the paste and the sand grains are called bond cracks. Secondly, there are microcracks in the cement paste extending perpendicular from sand grains, running dead in the paste, or bridging two sand grains. These microcracks are called paste cracks and have widths of 1–5 μm[1]. Figure 2a shows a micrograph of an impregnated microcrack passing a sand grain. It can be inferred from the image that debonding of the cement paste with the sand grain could have taken place in this case, without being visible as a bond crack.

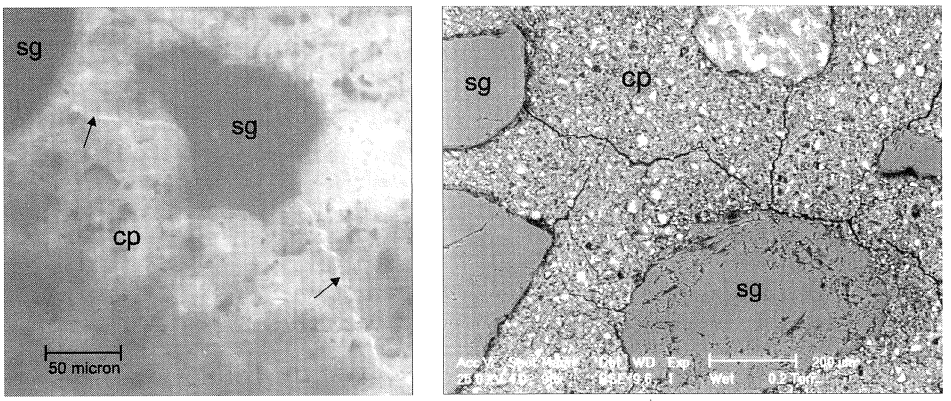

a. b.

Fig. 2. (a.) Paste microcrack(s) in a fluorescent thin-section of young mortar. No bond cracks are visible. (b.) Paste microcracks as seen in ESEM using the BSE-detector at 0.2 torr. Paste cracks are about perpendicular to sand grain boundaries. sg = sand grain; cp = cement paste.

3.2 *Appearance of microcracks in* ESEM

In the ESEM-sample the microcracks are not impregnated and normally show much more contrast with the surrounding material. When either the GSE- or the BSE-detector is used the cracks appear

[1] The crack width in this paper is defined as the average width of the visible part of the crack. In each mapping exercise a number of cracks widths were measured.

black, while the surrounding material is, in general, much lighter (see Figure 2b). In the ESEM also bond cracks and paste cracks (mostly perpendicular to sand grain boundaries) can be distinguished in the mortar. As in the thin-section, bond cracks are not always seen when it can be inferred from the structural context that debonding could have taken place. Besides, bond cracks are sometimes not visible due to effects from polishing. This is due to the fact that polishing causes depressions of the cement paste next to the much harder sand grains. When the sand grains have imbricated edges overlying the paste, the bond cracks are not visible at all.
In contrast with the thin-sections, paste cracks on different scales can be observed in the mortar in the ESEM due to the better resolution of the technique and the higher contrast of the microcracks. In the GSE-mode (at 5 torr, corresponding with r.h. of about 25% at room temperature) microcracks can be observed with crack widths in between 1 and 5 μm. Smaller microcracks are present too with widths of less then 0.5 μm (Figure 3). Also, it is often observed that the wider microcracks branch into finer microcracks (Figure 3).

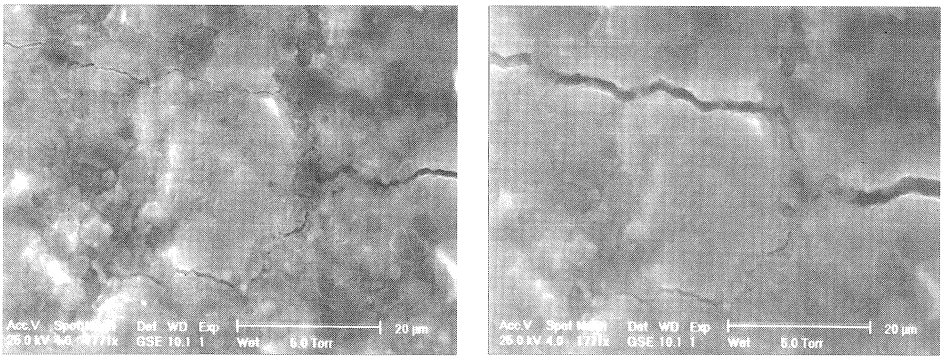

a. b.

Fig. 3. *(a.) Branched microcrack as seen in ESEM using the GSE-detector at 5 torr. (b.) Microcrack at same spot as in Figure 3a after drying at 0.2 torr. The upper part of the crack has opened.*

From the preliminary observations it became clear that no definite classification of paste cracks could be made on basis of crack width in the examined mortar samples.
It must be noted that the width of microcracks depends on the shrinkage behaviour of the cement paste in the ESEM. And this, in turn, depends on the relative humidity in the ESEM-chamber. This has been shown by Kjellsen and Jennings [7] for 8 months old high performance cement at relative humidities between 40% and 90%. Drying of the paste at r.h. of 40% resulted in opening of microcracks. The microcracks closed again during rewetting to r.h. of 90%. The ESEM-samples in this study were dried at r.h. of about 25% for two hours, during examination. When the pressure in the chamber was lowered to 0.2 torr in the BSE-mode (corresponding with a relative humidity of about 1% at room temperature), some of the microcracks opened within some minutes due to this drying (see Figure 3). Many microcracks can be observed with widths in between 3 and 8 μm with the BSE-detector at 0.2 torr (see Figure 2b). When the water vapour pressure in the chamber was increased

again to 5 torr, the cracks did not close, at least not within 1 hour. It is possible that cracks will not close at all, because local rotations near the crack face will prevent that the two crack faces will fit together.

3.3 *Microcrack mapping*

On basis of preliminary observations no definite microcrack classification, other than bond and paste cracks, could be made. One can decide to map all microcracks that can be seen with both techniques, but in this case the mapping has to be performed at high magnifications, and then the amount of work increases enormously. In this study it was decided to work at a constant magnification of 100× for the fluorescent thin-sections. In the GSE-mode microcracks are mapped at a monitor magnification of 450× and in the BSE- mode at 200×. All paste cracks that are seen at these magnifications are mapped. For thin-sections this means that cracks with a lower width limit of 1 μm are mapped. Using ESEM at the aforementioned magnifications, cracks having widths of more then 1 μm and 2 μm for the GSE- and BSE-modes, respectively, are detected. So, applying this method means that only cracks with a certain crack width range are mapped.

Besides the magnification it is also important to keep all other microscope settings constant, because they may also influence the image quality, and thus the resolution at a certain magnification.

The settings of the ESEM were: an acceleration voltage of 25 kV, a spot size 4, a working distance of 10 mm, and chamber pressures of 5 and 0.2 torr.

It was decided not to map the bond cracks because of the following reasons. As described in the previous paragraphs debonding could have taken place without being visible as a crack. Also, bond cracks are not always visible in ESEM due to polishing effects. Besides, it appeared that the observed bond cracks are always accompanied by paste cracks. For the purpose of this study, mapping of the visible bond cracks would not add significantly more information to the crack maps. In this study only the number and distribution of the paste microcracks are of interest. In the crack maps, each crack can thus be simplified as one straight black line, traced between the observed begin and end point of the crack.

Of each thin-section the middle part with a total area of 20×40 mm^2 is mapped; for an ESEM-sample only the middle square cm is mapped. Before mapping reference images are made of the mapped areas, using a stereomicroscope. These images are then used to map the cracks manually, when sitting behind the microscopes. After mapping the cracks they are digitized. To produce a digitized crack map of 800 mm^2 thin-section and 100 mm^2 of the ESEM-sample takes about $2\frac{1}{2}$ hours for both sample types.

4 Results and Discussion

Figure 4 shows microcrack maps obtained with fluorescence light microscopy (FLM). Figures 4a and b show one example of a crack map at both stages (i.e. 2 and 8 days curing respectively).

The number of microcracks in all three thin-section at the two hardening stages are given on top of the two crack maps. Figure 4c shows an example in which the crack map is combined with a micrograph of the grain structure of the mortar.

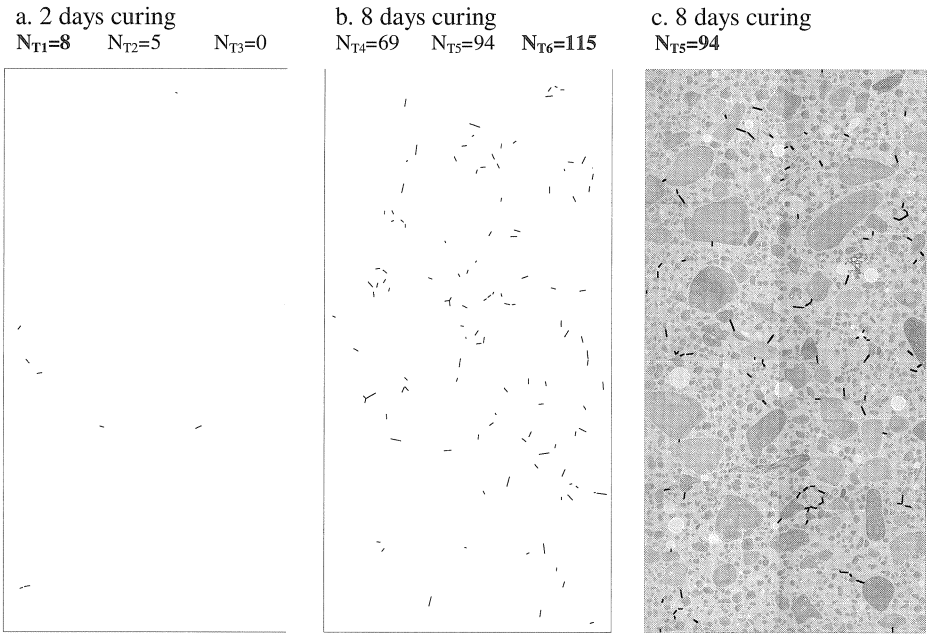

Fig. 4. Microcrack maps of 20 × 40 mm² on basis of fluorescent thin-sections. Microcracks that are mapped have widths of 1–5 μm. Figures (a.) and (b.) show maps for the two hardening stages (see section 2.2 for exact age). Figure (c.) shows a microcrack map combined with the reference image of the thin-section.

In Figure 5 microcrack maps of the two hardening stages in the mortar obtained with FLM and ESEM are compared. The FLM crack maps in this figure are the centers (9.5 × 9.5 mm²) of the maps given in Figures 4a and b. All crack maps in Figure 5 thus have the same position within the prism (see section 2.2). For the FLM and ESEM-GSE maps each time one example is given. The number of microcracks in the three crack maps at each stage are given on top of the maps. Only one map for both hardening stages was produced in the ESEM-BSE mode. The indices of the crack count refer to the number of the prism. For example, thin-section T1 and ESEM-sample E1 originate from the same prism.
From the thin-sections that were made with cuts perpendicular to the sample surface, it was observed that cutting did not introduce any additional cracks in the mortar at both hardening stages. At least not in the range of the mapped cracks, which is 1-5 μm for thin-sections. From this observation and on basis of observations that paste cracks have in general a perpendicular orientation to sand grain boundaries it can be concluded that the observed microcracks are caused by shrinkage of the cement paste restrained by the sand grains. This type of crack-patterns due to a shrinking paste has been predicted by Goltermann [9] on basis of the linear elasticity theory. It also follows from numerical analysis with the lattice model by Vervuurt and Van Mier [10].

The crack maps in Figures 4 and 5 show a clear increase in the number of cracks in the 8 day hardening stage compared with the 2 day stage. This increase can be explained by a higher magnitude of autogenous shrinkage after 8 days. Of the five types of shrinkage mentioned in the introduction, autogenous shrinkage probably only could have occurred internally in the mortar. A higher magnitude of autogenous shrinkage of cement paste at 8 days in comparison to the 2 day hardening stage, has been shown for a cement paste with w/c ratio of 0.4 by Tazawa [11].
When the FLM and ESEM-GSE crack maps are compared, it becomes clear that less microcracks are detected with FLM. This can be explained by the limited contrast of the cracks in the fluorescent thin-section: only part of the present microcracks are recorded. Another explanation could be that the ESEM-sample is overprinted by drying shrinkage in the ESEM at r.h. of about 25%, which causes cracks to open [7] and possibly creates new microcracks. This also happens when the ESEM-sample is dried at a r.h. of about 1%. The ESEM-BSE crack maps show much more and wider cracks than crack maps obtained at r.h. of about 25% in the GSE-mode.

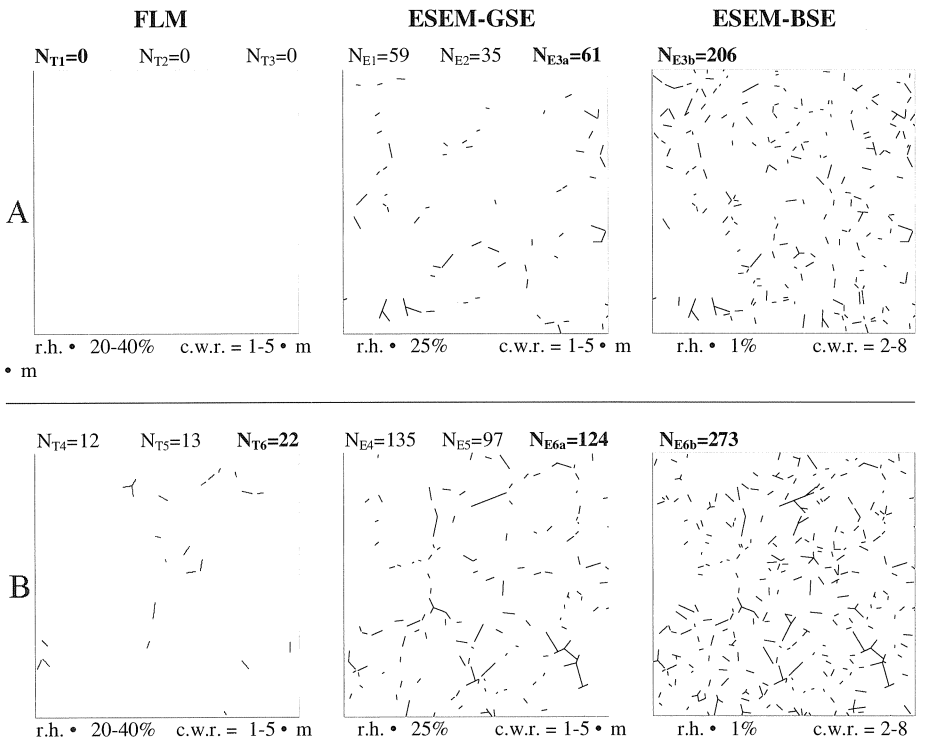

Fig. 5. Comparison of microcrack maps (9.5 × 9.5 mm²) obtained with different techniques at different relative humidities. A = the 2 days curing stage; B = the 8 days curing stage; r.h. = relative humidity; c.w.r. = crack width range.

5 Conclusions

From the preliminary results it can be concluded that microcrack mapping can be an aid to quantify shrinkage microcracking in young mortar. The microcrack maps may also give insight in possible preferred distributions of the microcracks. Preferred distributions within one crack map may be present, but also when different parts of a specimen are mapped, preferred distribution within a specimen can be found.
An important observation in this study is that microcracks open as a result of drying, which has also been shown by Kjellsen and Jennings [7]. The implication of these observations is that microcrack quantification at constant magnification should always be performed as function of the relative humidity during sample preparation (thin-sections) and the relative humidity during viewing (ESEM).

6 Acknowledgements

The assistance of Mr. A.S. Elgersma is gratefully acknowledged. Financial support was obtained from Delft Interfaculty Research Program 'Reliability of Constructions' (DIOC 10).

7 References

1 AÏTCIN, P.C., NEVILLE, A.M. and ACKER, P., Integrated view of shrinkage deformation. Con. Int., Vol.19, 1997, pp. 35-41.
2 RINGOT, E., OLLIVIER, J.P. and MASO, J.C., Characterisation of initial state of concrete with regard to microcracking. Cem. Con. Res., Vol.17, 1987, pp. 411-419.
3 GRAN, H.C., Fluorescent liquid replacement technique. A means of crack detection and water:binder ratio determination in high strength concretes. Cem. Con. Res., Vol.25, No.2, 1995, pp. 1063-1074.
4 OLLIVIER, J.P., A non destructive procedure to observe the microcracks of concrete by scanning electron microscopy. Cem. Con. Res., Vol.15, 1985, pp. 1055-1060.
5 BASCOUL, A., OLLIVIER, J.P. and TURATSINZE, A., Discussion of the paper 'Fracture zone presence and behaviour in mortar specimens' by N. Krstulovic-Opara. ACI Mat. J. Vol.91. No.5, 1994, pp. 531-533.
6 SUJATA, K. and JENNINGS, H.M., Advances in scanning electron microscopy. MRS bull. Vol.16, No.3, 1991, pp. 41-44.
7 KJELLSEN, K.O. and JENNINGS, H.M., Observations of microcracking in cement paste upon drying and rewetting by environmental scanning electron microscopy. Advn. Cem. Bas. Mat., Vol. 3, 1996, pp. 14-19.
8 Manual for grinding machine for the production of thin sections – *model DBT diamond roller grinder/86* – Dansk Beton Teknik A/S, Hellerup, Denmark.
9 GOLTERMANN, P., Mechanical predictions of concrete deterioration – Part 2: classification of crack patterns. ACI Mat. J. V.92, No.1, 1995, pp 58-63.

10 VERVUURT, A. and VAN MIER, J.G.M., Optical microscopy and digital image analysis of bond-cracks in cement-based materials, in *Microstructure of Cement-based Systems/Bonding and Interfaces in Cementitious Materials,* Diamond, S., et al., Eds., MRS, Pittsburgh, PA, 1995, 370, pp. 337-342.

11 TAZAWA, E. and MIYAZAWA, S., Influence of constituents and composition on autogenous shrinkage of cementitious materials. Mag. Con. Res., Vol.49, No.178, 1997, pp. 15-22.